

## Influence of the exchange potential on the neutron radius of $^{208}\text{Pb}$ extracted from sub-Coulomb pickup\*

J. W. Negele<sup>†</sup>

*Laboratory for Nuclear Science and Department of Physics,  
Massachusetts Institute of Technology, Cambridge, Massachusetts 02139*

(Received 1 November 1973)

Analysis of sub-Coulomb pickup using the realistic nonlocality arising from the exchange term in Hartree-Fock theory is shown to yield a point-nucleon rms radius for the excess neutrons in  $^{208}\text{Pb}$  of 6.21 fm, a value of 0.22 fm larger than previously obtained using local potentials. A simple schematic calculation is presented to elucidate the effect of nonlocality and arguments are presented to substantiate the reliability of a more realistic calculation. The implications of this result concerning the Coulomb energy anomaly are briefly discussed.

[ NUCLEAR STRUCTURE  $^{208}\text{Pb}(p, d)$ ,  $(d, t)$  calculated in Hartree-Fock theory;  
relation to Coulomb displacement energy. ]

Sub-Coulomb pickup provides one of the least ambiguous experimental constraints on the neutron distribution of  $^{208}\text{Pb}$  presently available.<sup>1, 2</sup> This constraint is, however, quite limited, specifying essentially only the absolute magnitude and exponential decay of the extreme tails of the last five neutron orbitals in the region of 15 fm. Hence, the purpose of this present note is to investigate the relation of the rms radii of the neutron wave functions to single-particle energies and the absolute magnitudes of the extreme tails in the context of a self-consistent Hartree-Fock theory which properly includes exchange.

### I. SCHEMATIC TREATMENT OF THE NONLOCAL EXCHANGE POTENTIAL

Before presenting the details of a realistic calculation, it is worthwhile to briefly consider a very schematic model which isolates the essential effect of the exchange potential on the spatial neutron distribution. In density-dependent Hartree-Fock (DDHF) theory based on a realistic two-body interaction, the dominant contribution to the single-particle potential is not the simple local Hartree term, but rather the exchange term.<sup>3</sup> Thus, the nonlocal exchange potential plays an essential role and cannot be neglected. Denoting the effective two-body interaction as  $v_{\text{eff}}$ , the Schrödinger equation for a particle in state  $\psi_j$ , may be written schematically as

$$\left[ -\frac{\hbar^2}{2m} \nabla^2 + \int d^3x' \sum_i |\psi_i(x')|^2 v_{\text{eff}}^{\text{dir}}(x' - x) - E_j \right] \psi_j(x) + \int d^3x' \sum_i \psi_i^*(x) \psi_i(x') v_{\text{eff}}^{\text{exch}}(x' - x) \psi_j(x') = 0. \tag{1}$$

In the interior of a nucleus, the density matrix  $\sum_i \psi_i^*(\vec{x}) \psi_i(\vec{x}')$  is very well approximated by the Slater mixed density which is the density matrix of a Fermi gas of plane waves at the interior density  $\rho^4$ :

$$\sum_i \psi_i^*(\vec{x}) \psi_i(\vec{x}') \approx \rho \rho_{\text{sl}}(k_F | \vec{x}' - \vec{x} |)$$

$$\rho_{\text{sl}}(\eta) = \frac{3j_1(\eta)}{\eta}$$

$$k_F = \left( \frac{3\pi^2}{2} \rho \right)^{1/3}.$$

Thus, in the nuclear interior the exchange term may be approximated:

$$\int d^3s \rho \rho_{\text{sl}}(k_F s) v_{\text{eff}}^{\text{exch}}(s) \psi_j(\vec{x} + \vec{s}).$$

Since the product  $\rho_{\text{sl}}(k_F s) v_{\text{eff}}^{\text{exch}}(s)$  is short range and spherically symmetric, we may expand  $\psi_j(\vec{x} + \vec{s})$  about  $\vec{x}$  to obtain

$$\left[ \int d^3s \rho \rho_{\text{sl}}(k_F s) v_{\text{eff}}^{\text{exch}}(s) \right] \psi_j(\vec{x}) + \left[ \int d^3s \rho \rho_{\text{sl}}(k_F s) v_{\text{eff}}^{\text{exch}}(s) \frac{s^2}{6} \right] \nabla^2 \psi_j(\vec{x}) + \dots$$

Thus, the first term may be grouped with the Hartree term in (1) and the second term may be regrouped with the kinetic energy term yielding a local Schrödinger equation with an effective mass  $m^*$  given by:

$$\frac{\hbar^2}{2m^*} = \frac{\hbar^2}{2m} - \int d^3s \rho \rho_{\text{sl}}(k_F s) v_{\text{eff}}^{\text{exch}}(s) \frac{s^2}{6}$$

In the interior of a large nucleus,  $m^*/m \sim 0.6$ .

The above argument may be straightforwardly generalized to include the nuclear surface,<sup>4</sup> resulting in a Schrödinger equation of the form:

$$\left(-\nabla \cdot \frac{\hbar^2}{2m^*(r)} \nabla + V(r) - E_j\right) \psi_j(r) = 0. \quad (2)$$

The position-dependent effective mass  $m^*(r)$  is  $\sim 0.6m$  in the nuclear interior and rapidly approaches  $m$  in the surface.

An illuminating caricature of such a position-dependent effective mass is a spherical square-well potential which has a constant value of  $m^*$  within the well and the true mass  $m$  outside. For a continuous  $m^*(r)$  the radial equation has the structure

$$\left\{ \frac{d}{dr} \frac{m}{m^*(r)} \frac{d}{dr} + \frac{2m}{\hbar^2} [E - V(r)] \right\} u(r) = 0, \quad (3)$$

where  $V(r)$  contains an additional term proportional to

$$\frac{1}{r} \frac{d}{dr} \frac{1}{m^*(r)},$$

as well as the usual centrifugal potential. In the limit of a discontinuous change in  $m^*(r)$ , two terms contribute to a discontinuity in the derivative of  $u(r)$  at the well edge: the term

$$\frac{d}{dr} \frac{m}{m^*(r)} \frac{d}{dr} u(r)$$

and a  $\delta$  function in the potential arising from

$$\frac{1}{r} \frac{d}{dr} \frac{1}{m^*(r)}.$$

This latter effect is a curvature correction which becomes negligible for large radii, as is also evident by noting that it would never occur if (2) were evaluated in Cartesian coordinates for a plane surface. Since it is straightforward to verify that both terms contribute to the discontinuity in  $u'(r)$  with the same sign and that the second derivative dominates, the qualitative effect of nonlocality may be most simply demonstrated by dropping the curvature term. Integration of radial Eq. (3) across the well boundary then yields the desired matching condition:

$$\int_{R-\epsilon}^{R+\epsilon} \frac{d}{dr} \frac{m}{m^*(r)} \frac{d}{dr} u(r) = \int_{R-\epsilon}^{R+\epsilon} \frac{2m}{\hbar^2} (V(r) - E) u(r),$$

or, since  $u(r)$  is continuous

$$\frac{m}{m^*(R^-)} \frac{u'(R^-)}{u(R^-)} = \frac{m}{m^*(R^+)} \frac{u'(R^+)}{u(R^+)}.$$

For the simple square well, we denote this interior potential as  $V$ , the eigenvalue as  $E$ , and

the interior ratio  $m^*/m \equiv \eta^2$ . Defining  $K = [(E - V)2m]^{1/2}$  and  $k = [(-E)2m]^{1/2}$ , the interior and exterior zero angular momentum solutions to be radial Eq. (3) are

$$u^-(r) = A \sin(\eta Kr), \quad u^+(r) = B e^{-kr},$$

and the matching condition becomes

$$\tan(\eta KR) = \frac{K}{\eta k}. \quad (4)$$

The absolute magnitude of the tail is obtained from the normalization condition

$$\frac{1}{B^2} = R e^{-2kR} \left[ \frac{\sin(2\eta KR)/2\eta KR - 1}{\cos(2\eta KR) - 1} + \frac{1}{2kR} \right]. \quad (5)$$

In the context of this simplified model, the information that would be specified in a sub-Coulomb pickup experiment determines the parameters  $E$  and  $B$ . For any given value of  $m^*/m \equiv \eta^2$ , it is then straightforward to solve for the corresponding well depth  $V$  and radius  $R$  and thus determine the wave function.

An illustrative case worked out on a hand calcu-

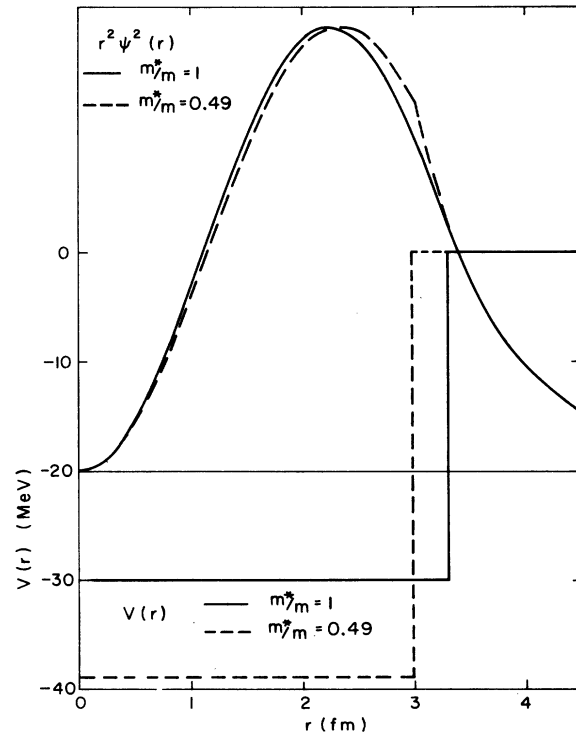


FIG. 1. Comparison of wave functions in the schematic effective mass model. The wave functions and potentials for  $m^*/m = 1$  and  $m^*/m = 0.49$  are denoted by solid and dashed curves, respectively. Both solutions were constrained to have  $E = 20$  MeV and the same absolute tail. Both wave functions are normalized but plotted on an arbitrary scale.

lator is graphed in Fig. 1. The potential and radial wave function squared for the local case  $m^*/m=1$  are denoted by solid lines, and correspond to the parameters  $E=20$  MeV,  $V=30$  MeV, and  $R=3.312$  fm. Requiring the same eigenvalue and exponential tail for  $m^*/m=0.49$  yielded the parameters  $V=38.96$  and  $R=2.984$ , and the corresponding solution is denoted by dashed curves. Thus, in this extreme model, the effect of nonlocality is to generate a cusp in the density at the surface, with a corresponding depletion of the interior density as required by normalization. The behavior is qualitatively the same when the surface contribution in the potential is included and when radial nodes or higher angular momentum states are treated. The analogous behavior for a continuous potential may be explored with the Skyrme force<sup>5</sup> which will be treated in detail subsequently. In this case, the discontinuous cusp is replaced by a smoothed distribution which still displays the same increased density near the maximum slope of the potential for the nonlocal case and a compensating decrease of the interior density required by normalization.

The behavior demonstrated in Fig. 1 is closely related to the so-called "Perey effect"<sup>6</sup> in which the nonlocal scattering wave function is consistently smaller than the corresponding local wave function inside the nuclear optical potential. The essential difference between bound states and scattering states is that by normalization, the bound-state wave functions cannot decrease everywhere and without the preceding calculation, it was not completely obvious where the increase would actually occur. The general feature which should be emphasized in this schematic calculation is that a local and nonlocal wave function constrained to have identical single-particle energies and tails differ in that the nonlocal wave function has a higher density at the surface of the potential and a correspondingly lower density in the interior. Hence, the rms radius of the nonlocal wave function is systematically larger than that of the local wave function. We will demonstrate below that this feature persists in much more realistic calculations.

## II. REALISTIC CALCULATIONS

Ideally, it would be desirable to calculate the neutron tails with a theory which is derived from the two-body nucleon-nucleon interaction and which exactly reproduces the binding energy, single-particle energies, and charge form factor of  $^{208}\text{Pb}$ . The DDHF theory of Refs. 3 and 4 falls short of this ideal in two respects, one theoretical and one experimental. First, theoretically,

it contains two parameters which, although calculable in principle, have not yet been calculated from the two-body force. Fortunately these parameters have negligible effect on the nonlocality of the single-particle potential, which is essentially specified by the size of the "Fermi hole"  $\sim \pi/k_F$  and the long-range part of the effective two-body interaction. Rather, these parameters describe the contributions to saturation by higher-order terms in perturbation theory which require that particles be extremely close spatially and are in fact approximated by a zero-range potential. In the separation effected in Ref. 4, these free parameters affect only the nuclear matter binding energy functional  $V^{nm}(\rho_n, \rho_p)$  while the effective mass arises from the functional  $B(\rho_n, \rho_p)$  which is uniquely determined from the two-body force. Experimentally, although systematic qualitative agreement with single-particle energies and charge radii is obtained, slight discrepancies in single-neutron energies and the charge radius exist in  $^{208}\text{Pb}$  which must be examined in this present application. The charge radius for point protons using the density matrix expansion (DME) wave functions of Ref. 4 is 5.451, which is 0.014

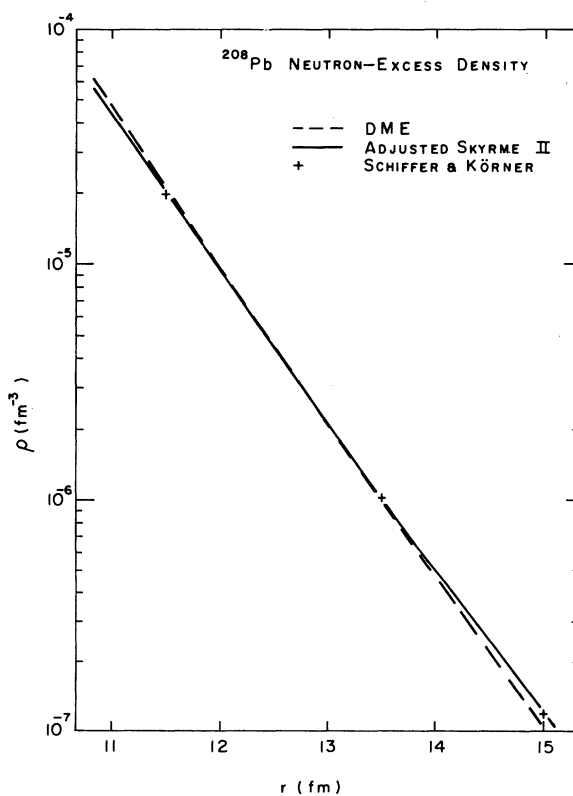


FIG. 2. Comparison of neutron excess densities for point nucleons in the extreme tail. The three calculations are discussed in detail in the text.

fm smaller than the value extracted from electron scattering and muonic x rays.<sup>7</sup> Thus, one would expect the neutron surface to be displaced inward by roughly 0.01–0.02 fm. This displacement is quite small compared with the effect of nonlocality on the radius of the neutron excess which is on the order of 0.2 fm.

The DME single-neutron energies are on the average 1 MeV overbound, and this constitutes a much more serious discrepancy. As pointed out by Körner and Schiffer,<sup>1</sup> this error implies asymptotic tails which decay too rapidly and therefore eventually must drop below the experimental density. To ascertain whether this error has begun to dominate in the region of 11 through 15 fm, the DME neutron density is plotted in Fig. 2 (dashed curve) and compared with the density reconstructed from experiment by Schiffer and Körner<sup>2</sup> (denoted by crosses). In this figure, one observes that indeed even in this region the DME neutron slope is perceptibly steeper than the experimental one. However, the absolute discrepancy is again small on the scale of 0.2 fm, so there is reason to expect that a theory adjusted to give the proper slope will not differ significantly.

In order to conveniently adjust the effective interaction to remedy the two discrepancies cited above, we now use the Skyrme interaction,<sup>5</sup> which may be regarded as a simple parametrization of the interaction derived in the DME. Aside from the spin-orbit potential, the Skyrme interaction has five parameters. Four constraints on these parameters are provided by the volume energy, Coulomb energy (or alternatively the charge radius), surface energy, and symmetry energy reflected in the nuclear masses. Thus, there is one essentially undetermined parameter which corresponds to the effective mass in nuclear matter. Two different Skyrme interactions are particularly relevant to this present work. The Skyrme II inter-

action has the value  $m^*/m = 0.58$  which is consistent with the nuclear matter result, and the Skyrme I force has  $m^*/m = 0.91$  which is close to the result one would obtain in a pure Hartree theory which totally neglects the nonlocal exchange interaction. Both interactions have the remaining four parameters adjusted to roughly fit the energies and radii of spherical nuclei. Thus, with very minor adjustment of the parameters in Ref. 5, it is possible to remedy the two specific shortcomings of the DME in <sup>208</sup>Pb and thereby compare the neutron radii extracted from two theories which have a realistic nonlocality and essentially no nonlocality, and which fit the required properties of <sup>208</sup>Pb.

One technical difficulty still remains, because even including the spin-orbit potential it is impossible to simultaneously fit the removal energies of the last five neutron orbitals. However, the most essential feature is that the neutron density have the proper slope, which only requires that the weighted average of the single-particle energies agree with the same average of the experimental energies. In performing this average, we clearly sacrifice the additional information that would be provided by knowing the absolute amplitudes of the individual wave functions. However, in principle this additional information is somewhat illusory, since configuration mixing should occur between the neutrons in the last five orbitals and the analysis assumed spectroscopic factors of unity.

In the calculations with Skyrme II, it turned out to be sufficient to simply vary the parameter  $t_3$ , which specifies the repulsive density dependence, until the point proton rms radius agreed with the experimental value 5.465. The results are tabulated in Table I and the neutron-excess density is plotted in Fig. 2 (solid curve). As seen from the graph, the slope of the exponential turned out quite

TABLE I. Comparison of local and nonlocal results. The symbols  $r_p$ ,  $r_{ne}$ , and  $r_n$  denote the point-nucleon rms radii for protons, excess neutrons, and all neutrons, respectively. The direct Coulomb energy of the neutron excess assuming point nucleons is denoted  $E_{\text{Coulomb}}$ , and  $\rho_{\text{exp}}(11.5)$  refers to the value extracted in Ref. 2.

	$r_p$ (fm)	$r_{ne}$ (fm)	$r_n - r_p$ (fm)	$t_3$ Original (MeV fm <sup>6</sup> )	$t_3$ Adjusted (MeV fm <sup>6</sup> )	BE/A (MeV)	$E_{\text{Coulomb}}$ (MeV)	$\frac{\rho_{ne}(11.5)}{\rho_{\text{exp}}(11.5)}$
DME	5.451	6.208	0.20			7.835 <sup>a</sup>	18.79	1.09
Skyrme II	5.465	6.206	0.20	9331.	9131.1	7.809	18.76	1.03
Skyrme I	5.465	5.980	0.12	14 463	15 073.5	7.341	19.20	0.96
(exp)	5.465		(0.21 ± 0.13) <sup>b</sup>			7.87	(20.03) <sup>c</sup>	
Körner-Schiffer	5.45	5.99						

<sup>a</sup> For comparison with the Skyrme results, the starting energy corrections of Ref. 2 are omitted.

<sup>b</sup> The value given in Ref. 12 has been corrected by using the preferred value  $r_p = 5.465$ .

<sup>c</sup> This value includes the corrections from Refs. 9 and 10 explained in the text.

satisfactorily, with the  $p$  states being 0.3 MeV underbound, the  $i_{13/2}$  state exactly correct, and the  $f$  states 1 MeV overbound. One observes that this calculation yields excellent agreement with the measured density at 15 fm, certainly within the errors associated with the neglect of finite range and the assumption of unit spectroscopic factors. However, the rms radius of the neutron excess is 0.22 fm larger than inferred from the local analysis of Ref. 1, also recorded in Table I. The close agreement between the DME and Skyrme II entries in Table I confirms our earlier conjecture that the slight discrepancies in rms radius and average single-particle energy in the DME would not introduce significant errors on the scale of 0.2 fm. Therefore, we find it most meaningful to compare in Table I the neutron-excess density with the value at 11.5 fm reconstructed from the experimental data, since calculations which differ only by minor changes in the asymptotic tail are essentially indistinguishable at 11.5 fm.

To conclusively prove that the significant shift of 0.22 fm is the result of nonlocality and not some other feature of the DME and Skyrme theories, we attempted to adjust Skyrme I to reproduce the exact proton rms radius and average single-particle energy. In this case, varying  $t_3$  to yield the proper proton radius resulted in a slight underbinding on the average. Hence, although the density agreed well with the "experimental" one at 11.5 fm, it gradually rose well above the value at 15 fm. Variation of the other Skyrme parameters to improve the single-particle energies while keeping the proton radius fixed has the undesirable property of decreasing  $m^*/m$ . Whereas to a theorist who firmly believes  $m^*/m$  should be 0.6 this may be reassuring, it tended to obliterate the point of the calculation which was to simulate a local Hartree theory. Undoubtedly, by introducing additional parameters in the force, one could force  $m^*/m$  to remain close to one while fitting the single-particle energies, but we have not attempted to do so. Rather, observing from the DME-Skyrme II results that correcting the extreme tail has negligible effect on the rms radii and Coulomb energy of the neutron excess, we simply present these results with the adjusted Skyrme I force in Table I. It is especially reassuring that the rms radius of the neutron excess in this calculation agrees so well with results of Ref. 1. The evidence thus strongly confirms the conclusion that analysis of the same sub-Coulomb pickup data with a theoretically realistic nonlocality increases the inferred neutron radius by 0.22 fm over the result obtained from a purely local potential.

### III. RELATION TO PREVIOUS WORK

The most salient feature of our results, that the rms radii of nonlocal solutions are systematically larger than those of local solutions, requires some discussion in view of the relative model independence demonstrated in the analysis of Körner and Schiffer. In particular, since it is always possible to reduce a nonlocal potential to a state-dependent local potential, it is useful to show why we obtained a shift much larger than seemed possible with the Woods-Saxon parametrization explored in their work.

In the analysis of Ref. 2, for a given diffuseness  $a$ , the depth  $V_0$  and well radius  $R$  were determined such that the eigenvalue and magnitude of the tail at 15 fm were exactly reproduced. The rms radii of the wave functions were then explored as a function of the diffuseness  $a$ , with the results presented in their Table II. The low angular momentum states display the intuitively obvious behavior that the rms radii increase significantly with increasing diffuseness. The high angular momentum states, however, show an almost exactly compensating decrease in rms radius. This seemingly unintuitive behavior becomes obvious if one plots the change in the total potential, including the large angular momentum barrier. Then increasing  $a$  with a compensating increase in  $V_0$  and decrease in  $R$  to keep the tail and eigenvalue fixed weakens the repulsion near the origin as well as the intermediate attraction in such a way that the wave function on the average is pulled in. Thus, their insensitivity results from the cancellation brought about by assuming that the diffuseness is the same for all states.

There is no fundamental reason, however, why the diffuseness of the equivalent state-dependent potential should be the same for all states. Indeed, from the graphs of the equivalent local potentials for neutrons in Fig. 21 of Ref. 3 it is evident how to reconcile the diffuseness dependence of Ref. 2 with our result that nonlocality increases the rms radii for all wave functions. For the  $2p$  states the diffuseness is quite high, roughly  $a \sim 0.84$  and for low angular momentum, the rms radius increases with increasing diffuseness. For the high  $l$  states,  $0h$  and  $0i$ , the diffuseness is much lower, roughly 0.64, and for these states a decrease in diffuseness corresponds to an increase in radius. Thus, a crucial feature of the state dependence of the equivalent local potential is the inverse dependence of the diffuseness on the angular momentum.

### IV. IMPLICATIONS CONCERNING THE COULOMB ENERGY ANOMALY

Coulomb energy differences between mirror nuclei and displacement energies of isobaric ana-

log states have received considerable attention as possible sources of information concerning neutron radii.<sup>8</sup> An apparent anomaly has arisen in the analysis of Coulomb energies, since the radii of neutron excesses required to fit experimental energies are systematically on the order of 10–20% smaller than expected from reasonable theories. Since this present work indicates that analysis of sub-Coulomb pickup with a realistic nonlocality yields substantially larger neutron radii, it is useful to briefly discuss how this affects the interpretation of Coulomb energies.

In Ref. 1 there was still some hope that the radii extracted from pickup- and analog-state displacement energies could be reconciled. Analysis of the Coulomb displacement energy in <sup>208</sup>Pb including the direct Coulomb energy, the exchange Coulomb energy, the finite proton size, and the electromagnetic spin-orbit interaction<sup>8</sup> yield a point-neutron-excess radius of 5.90 fm, whereas sub-Coulomb pickup results yielded 5.99 fm.<sup>1</sup>

Subsequent analysis of contributions to the displacement energy in Pb, however, significantly reduces the inferred neutron-excess radius. The combined effect of vacuum polarization, two-body correlations, compound mixing, isospin mixing, dynamic *n-p* mass difference, and charge dependence estimated in Refs. 9 and 10 yield a shift of roughly -0.65 MeV which must be compensated by a decrease in the neutron radius to raise the direct Coulomb energy by 0.65 MeV. In addition, Lane<sup>11</sup>

has estimated that a substantial further decrease in the radius must be introduced to compensate the effect of second-order Coulomb interactions. To be conservative, we shall only include the -0.65-MeV shift and point out that this shift alone requires a point-neutron-excess radius of 5.52 fm.

Comparison with the present point-neutron-excess radius value of 6.21 obtained from the non-local analysis of sub-Coulomb pickup indicates an extremely serious discrepancy of approximately 0.7 fm, rendering the above interpretation of the Coulomb displacement energy irreconcilable with sub-Coulomb pickup.

Our present opinion is that the theoretical neutron wave functions with a neutron-excess radius 6.21 fm are in excellent agreement with the sub-Coulomb pickup data, as well as agreeing with the  $\alpha$ -scattering analysis of Ref. 12. Since, in addition, the theory yields proton densities which describe the systematics of electron scattering throughout the Periodic Table, there is very solid evidence that the theoretical wave functions are indeed correct and that the discrepancy with the radius extracted from the analog-state displacement energy must result from an error in the interpretation of that experiment. The most promising mechanism to resolve the anomaly still appears to be charge asymmetry. From Table I, this present analysis suggests that charge asymmetry must contribute roughly 1.3 MeV to the displacement energy.

\*Work supported in part through funds provided by the Atomic Energy Commission under Contract No. AT-(11-1)-3069.

†Alfred P. Sloan Foundation Research Fellow.

<sup>1</sup>H. J. Körner and J. P. Schiffer, *Phys. Rev. Lett.* **27**, 1457 (1971).

<sup>2</sup>J. P. Schiffer and H. J. Körner, *Phys. Rev. C* **8**, 841 (1973).

<sup>3</sup>J. W. Negele, *Phys. Rev. C* **1**, 1260 (1970).

<sup>4</sup>J. W. Negele and D. Vautherin, *Phys. Rev. C* **5**, 1472 (1972).

<sup>5</sup>D. Vautherin and D. M. Brink, *Phys. Rev. C* **5**, 626 (1972).

<sup>6</sup>F. G. Perey, in *Direct Interactions and Nuclear Reac-*

*tion Mechanisms*, edited by E. Clementel and C. Villi (Gordon and Breach, New York, 1963), p. 125.

<sup>7</sup>J. L. Friar and J. W. Negele, *Nucl. Phys.* **A212**, 93 (1973).

<sup>8</sup>J. A. Nolen, Jr., and J. P. Schiffer, *Phys. Lett.* **29B**, 396 (1969); and *Annu. Rev. Nucl. Sci.* **19**, 471 (1969).

<sup>9</sup>N. Auerbach, J. Hüfner, A. K. Kerman, and C. M. Shakin, *Phys. Rev. Lett.* **23**, 484 (1969).

<sup>10</sup>J. W. Negele, *Nucl. Phys.* **A165**, 305 (1971).

<sup>11</sup>A. M. Lane, in *Proceedings of the Symposium on Correlations in Nuclei*, Balatonfüred, Hungary, 1973 (unpublished).

<sup>12</sup>A. M. Bernstein and W. A. Seidler, *Phys. Lett.* **39B**, 583 (1972).